Available online at www.sciencedirect.com
SCIENCE DIRECT®
Biochimica et Biophysica Acta 1655 (2004) 102–115
BIOCHIMICA ET BIOPHYSICA ACTA
BBA
www.bba-direct.com

Review

Surface-mediated proton-transfer reactions in membrane-bound proteins

Pia Ädelroth*, Peter Brzezinski

Department of Biochemistry and Biophysics, The Arrhenius Laboratories for Natural Sciences, Stockholm University, Svante Arrhenius väg 12, SE-106 91 Stockholm, Sweden

Received 22 October 2003; accepted 22 October 2003

Abstract

As outlined by Peter Mitchell in the *chemiosmotic theory*, an intermediate in energy conversion in biological systems is a proton electrochemical potential difference (''proton gradient'') across a membrane, generated by membrane-bound protein complexes. These protein complexes accommodate proton-transfer pathways through which protons are conducted. In this review, we focus specifically on the role of the protein–membrane surface and the surface–bulk water interface in the dynamics of proton delivery to these proton-transfer pathways. The general mechanisms are illustrated by experimental results from studies of bacterial photosynthetic reaction centres (RCs) and cytochrome *c* oxidase (C*c*O).

Keywords: Proton pathway; Cytochrome *c* oxidase; Reaction centre; Photosynthesis; Respiration; Electron transfer; Kinetics

1. Introduction

Proton-transfer reactions from water solution to a protein and from a donor to an acceptor within a protein are among the most common reactions in biological systems (for a recent general review, see Ref. [1]). In this review, we focus on the role of the protein surface in facilitating proton uptake from solution to proton-transfer pathways of membrane-bound proteins, where the discussion is centred around experimental observations from studies of bacterial photosynthetic reaction centres (RCs) and cytochrome *c* oxidase (C*c*O).

The protonation rate of a base in a water solution, determined by proton diffusion in water, was shown to display second-order rate constant of $2–6 \times 10^{10}$ M^{-1} s^{-1} [2–6], reaching a limiting value for the recombination of OH^- and H^+ at 1.4×10^{11} M^{-1} s^{-1} [2]. The significance of the subject discussed in this review is illustrated by observations of proton uptake from solution by the RC and C*c*O with apparent bimolecular rate constants exceeding those corresponding to proton diffusion through water to a single surface-bound protonatable group. Such rapid proton-transfer reactions are presumably the consequence of the involvement of surface-exposed protonatable residues, which capture protons from solution thereby extending the surface area from which protons are collected and providing a local, two-dimensional buffer composed of rapidly exchanging protonatable sites [5,7]. For example, if negatively charged residues are combined with histidine residues with appropriate pK_A values, this type of structure may act to: (a) increase the local proton concentration around the entry point of the proton-transfer pathway, (b) bind protons from solution and ''funnel'' them to the pathway entrance, or (c) provide suitable bases for abstracting protons from buffers or from water molecules in solution. Rapid proton uptake from solution may be important for, e.g., stabilising transiently formed reduced states of intraprotein redox cofactors, stabilising partly reduced substrates or, in the case of proton pumps, protonating intraprotein residues involved in proton pumping where accurate timing of the protonation reaction is key to maintaining a high proton-pumping stoichiometry.

Abbreviations: RC, bacterial photosynthetic reaction centre; C*c*O, cytochrome *c* oxidase; Amino-acid residue numbering, e.g. Glu(I-286)/Glu(L-212) denotes the glutamic acid at position 286/212 in subunit I/L, for C*c*O (*Rhodobacter sphaeroides* C*c*O numbering)/RC (*R. sphaeroides* RC numbering)

* Corresponding authors. Pia Ädelroth is to be contacted at Tel.: +46-8-164183; fax: +46-8-153679. Peter Brzezinski, Tel.: +46-8-163280; fax: +46-8-153679.

E-mail addresses: piaa@dbb.su.se (P. Ädelroth), peterb@dbb.su.se (P. Brzezinski).

0005-2728/$ - see front matter © 2004 Elsevier B.V. All rights reserved.
doi:10.1016/j.bbabio.2003.10.018

1.1. Cytochrome c oxidase

Cytochrome *c* oxidase is a membrane-bound redox-driven proton pump. The C*c*O from *Rhodobacter sphaeroides* consists of four subunits (SU) of which SU I and II bind four redox-active cofactors, two copper sites and two haem groups (Fig. 1). Electrons are donated by a water-soluble cytochrome *c*, which interacts with C*c*O on the positive (P-) side of the membrane and first reduces the copper A (Cu_A) site. The electron is then transferred intramolecularly consecutively to a haem group, haem *a*, and to a binuclear haem-copper centre consisting of haem a_3 and copper B (Cu_B), located within the membrane-spanning part of the C*c*O (Fig. 1B). When this binuclear centre is

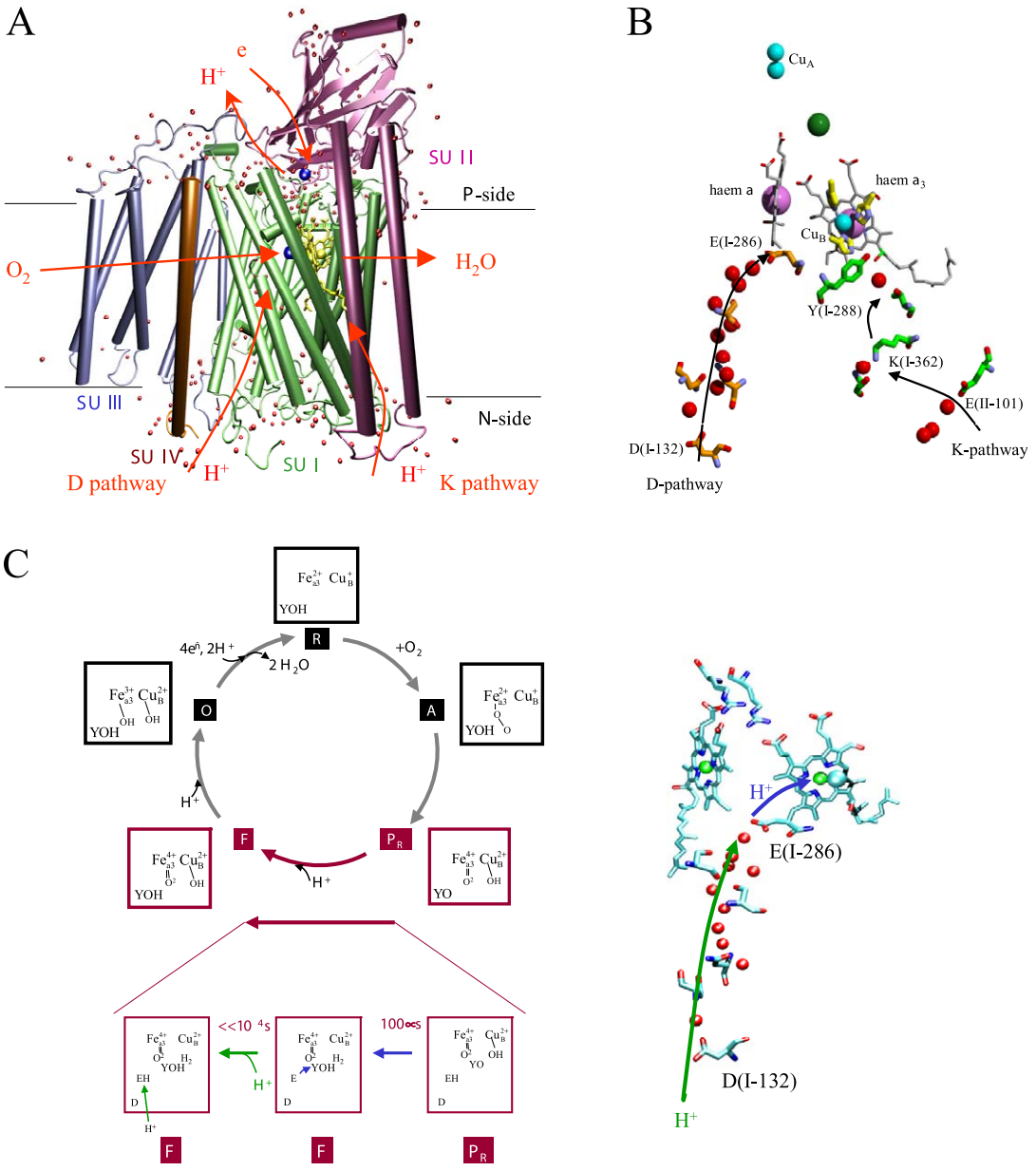

Fig. 1. (A) The overall structure of cytochrome *c* oxidase (C*c*O) from *R. sphaeroides* (PDB code 1 M56 [84]). The redox centres are shown in yellow (haems *a* and a_3) and blue (Cu_A and Cu_B). (B) The redox centres and the proton-transfer pathway of C*c*O. The D pathway is used for the uptake of both substrate and "pumped" protons. The red spheres are water molecules. (C) The reaction mechanism of C*c*O as observed upon mixing of the fully reduced C*c*O with O_2. Reduction of the oxidised (state **O**) C*c*O (with four electrons) is associated with a net uptake of about two protons from the bulk solution forming state **R**. Oxygen binds to the reduced haem a_3 (state **A**) with a time constant of ~10 μs (1 mM O_2). The breaking of the O–O bond forming state $\mathbf{P_R}$ is associated with electron transfer from haem *a* to the binuclear centre. The $\mathbf{P_R} \rightarrow \mathbf{F}$ and $\mathbf{F} \rightarrow \mathbf{O}$ transition are associated with proton uptake from the bulk solution. The proton-transfer reactions through the D pathway (shown to the right), associated with the $\mathbf{P_R} \rightarrow \mathbf{F}$ transition (discussed in this review), are shown in detail (in red boxes). The structural figures were prepared using the Visual Molecular Dynamic Software [85].

reduced, dioxygen is bound and reduced stepwise by four electrons to yield two water molecules. The protons needed for the O_2-reduction reaction (substrate protons) are taken up specifically from the negative (N-) side of the membrane. In addition, the reaction catalysed by C*c*O is coupled energetically to the pumping of protons from the N- to the P-side of the membrane with an average stoichiometry of one proton per electron (for a detailed description of the structure and function of C*c*O, see [8–13], and other articles in this issue):

$$4c_P^{2+} + 8H_N^+ + O_2 \rightarrow 4c_P^{3+} + 4H_P^+ + 2H_2O \quad (1)$$

where *c* is cytochrome *c*, and the subscripts N and P refer to the negative and positive sides of the membrane, respectively. The involvement of specific amino acid residues in

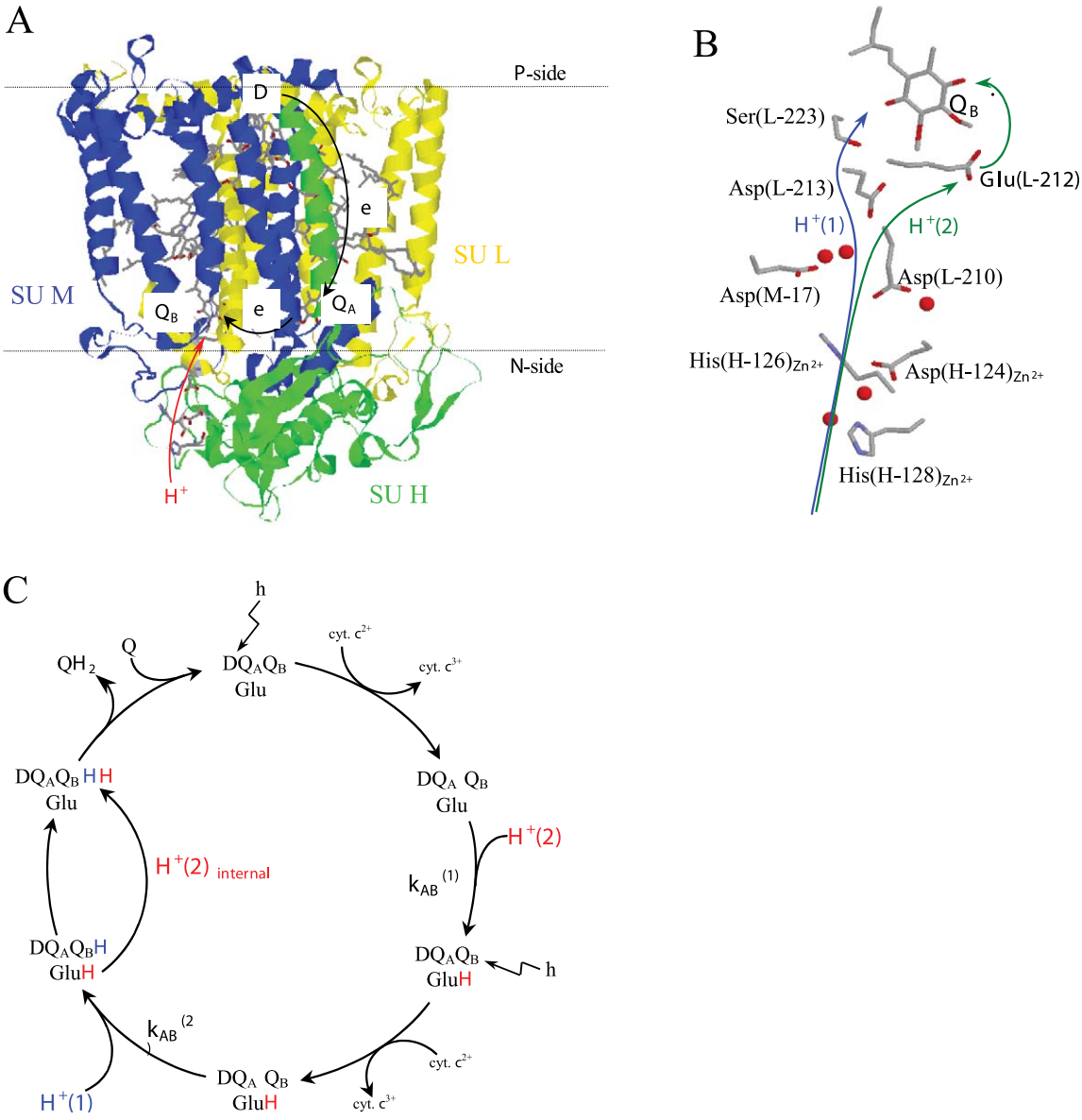

Fig. 2. (A) Overall structure of the reaction centre (PDB code 1AIG [86]), indicating the redox cofactors, the sequence of electron transfer and the pathway for proton transfer to the Q_B site. (B) The proton-transfer pathways for $H^+(1)$ and $H^+(2)$ to reduced Q_B. $H^+(2)$ is taken up (during $k_{AB}^{(1)}$) first to Glu(L-212) and is later (after $H^+(1)$ during $k_{AB}^{(2)}$) transferred on to reduced Q_B. Note that $H^+(1)$ and $H^+(2)$ share proton-entry point, at His(H-126) and His(H-128). The subscript Zn^{2+} indicates the residues that were shown to constitute the Zn^{2+}-binding site [28]. (C) A simplified photocycle for the reaction centre at pH>8. Light excitation leads to oxidation of the chlorophyll donor D and reduction of the primary quinone Q_A. D^+ is rapidly re-reduced by a cytochrome *c*. The first electron transfer from Q_A^- to Q_B, $k_{AB}^{(1)}$, is coupled to protonation (uptake of $H^+(2)$) of a nearby group, Glu(L-212). The second light-excitation leads to a second electron transfer from Q_A^- to Q_B, $k_{AB}^{(2)}$, which is coupled to direct protonation (uptake of $H^+(1)$) of the doubly reduced Q_B. After $k_{AB}^{(2)}$, $H^+(2)$ is transferred internally from Glu(L-212) to $[Q_BH]^-$, forming quinol, QH_2, which dissociates from the Q_B-binding pocket and is replaced by a quinone, Q.

these proton-transfer reactions have been investigated using site-directed mutagenesis in a number of bacterial C*c*Os of which the structure and function are essentially identical to those of the mitochondrial C*c*O. In cytochrome aa_3 from *R. sphaeroides* there are two proton-transfer pathways leading from the N-side towards the binuclear centre (see Fig. 1B). One of these, the so-called D-pathway, starts with a highly conserved Asp residue (Asp(I-132)) in the *R. sphaeroides* C*c*O), and is lined by a number of hydrophilic amino-acid residues and water molecules, leading to another highly conserved residue, Glu(I-286) (Fig. 1B). The D-pathway is presumably used for the transfer of at least six out of the eight protons (four substrate and four pumped protons) taken up by the C*c*O per each turnover [14–17]. Since the C*c*O catalyses the reduction of ~ 400 O_2 molecules/s at pH 6.5, on average ~ 2400 H^+/s are taken up through the D-pathway, corresponding to an average protonation rate constant of ~ g10^{10} M^{-1} s^{-1}. However, as discussed in detail below, many of the partial proton-uptake reactions are much faster than the average rate.

1.2. Bacterial photosynthetic reaction centers

The RC from the photosynthetic bacterium *R. sphaeroides* is a membrane-bound protein complex that catalyses the light-induced, proton-coupled electron transfer reactions leading to the two-electron reduction and double protonation of a bound quinone molecule Q_B, using electrons from cytochrome c_2 (reviewed in Refs. [18–20]).

$$Q + 2e^- + 2H^+ \rightarrow QH_2 \quad (2)$$

The RC (Fig. 2A) is composed of three polypeptide subunits, called L, M, and H. Light absorbed by the RC initiates the photo-ionisation of the primary donor, D, a bacteriochlorophyll dimer. The electron is transferred through a bacteriochlorophyll and a bacteriopheophytin to the primary quinone acceptor, Q_A, which is the electron donor to Q_B. The protons required for the reduction of the Q_B to quinol are taken up from the aqueous phase on the cytoplasmic side (N-side) of the membrane. The oxidised chlorophyll donor D^+ is re-reduced by a water-soluble cytochrome c_2 on the opposite side (P-side) of the membrane.

The double reduction of Q_B takes place in two sequential light-induced electron transfer reactions (see Fig. 2C). The first electron transfer from Q_A^- to Q_B, $k_{AB}^{(1)}$, produces a stable anionic semiquinone radical Q_B^-. At pH>8, no protonation of the semiquinone occurs at this step (the pK_A of Q_B^- has been estimated to be ~ 4.5 [21]), but the electron transfer is coupled to protonation of a nearby acid residue Glu(L-212) [22,23] due to electrostatic interaction with Q_B^-. The first protonation of the reduced Q_B (this proton is denoted $H^+(1)$) occurs during the second electron transfer, $k_{AB}^{(2)}$. The second proton (denoted $H^+(2)$) is transferred internally to $(Q_BH)^-$ from Glu(L-212) after the second electron transfer, $k_{AB}^{(2)}$ [24], forming Q_BH_2.

The Q_B molecule is located in the interior of the RC, removed from the aqueous solution. Several putative proton-transfer pathways consisting of protonatable amino acids and/or water molecules leading from the cytoplasm to the quinone-binding site have been identified in the crystal structures of the RC from *R. sphaeroides* [25–27].

The dominant functional proton-transfer pathway for $H^+(1)$ (Fig. 2B) has been shown by site-directed mutagenesis and metal-binding studies (see below) to involve the following residues, starting at the surface of the protein and moving 'in' towards the Q_B-site (see Fig. 2B): His(H-126), His(H-128) and Asp(H-124) (all three at the protein surface) [28,29], Asp(L-210) and Asp(M-17) [30,31], Asp(L-213) [22,32–34], and Ser(L-223) [32]. The transfer of $H^+(2)$ (Fig. 2B) to reduced Q_B has been shown by site-directed mutagenesis to involve internal transfer from Glu(L-212) [22,23]. The transfer of $H^+(2)$ from the bulk solution to Glu(L-212) has been shown to involve the same pathway as for $H^+(1)$ up to Asp(L-213) [31,35], before branching off to Glu(L-212).

The turnover steady-state activity of the RC has been measured to be ~ 1500 e^-/s at pH 8 [36], which corresponds to an average protonation rate constant of 1.5×10^{11} M^{-1} s^{-1}, and as discussed below, partial reactions involving proton uptake are even faster.

2. Rapid proton uptake reactions by C*c*O and photosynthetic RCs

2.1. Cytochrome c oxidase

Fully reduced (i.e., with four electrons) C*c*O reacts with dioxygen to form the oxidised C*c*O with a time constant of ~ 1 ms (at pH 7 and O_2 concentrations of >10 μM). However, as indicated above, the O_2-reduction reaction takes place in several distinct steps. These steps can be resolved in time using the "flow-flash technique"; the reduced C*c*O with CO bound at haem a_3 is mixed rapidly (a few ms) with an O_2-saturated solution. Since also O_2 binds initially to haem a_3, the reaction of the reduced binuclear centre and O_2 is rate-limited by the CO dissociation, which is a slow reaction displaying a time constant of ~ 50 s. Thus, if after mixing of the CO-bound C*c*O with O_2, the CO ligand is dissociated by means of a laser flash, the reaction of the reduced C*c*O and O_2 can be followed in time using, for example, optical absorption spectroscopy (for a review, see Refs. [37–39]). After binding of O_2 to haem a_3 in the fully reduced C*c*O, the three redox sites haem *a*, haem a_3 and Cu_B become oxidised resulting in formation of the so-called "peroxy" ($\mathbf{P_R}$) transient state. The $\mathbf{P_R}$ state appears with a time constant of 30–50 μs and results in formation of a proton acceptor at the catalytic site having a very high pK_A (>12). The group is presumably

either a Tyr residue, which donates a proton to O_2 upon formation of $\mathbf{P_R}$ or a hydroxide bound at Cu_B after the breaking of the O–O bond (see Fig. 1C), but the discussion below is independent of the identity of the group. Reprotonation of this group displays a time constant of ~ 100 μs at pH 7 and results in the formation of the **F** state. Thus, the $\mathbf{P_R} \rightarrow \mathbf{F}$ transition can be viewed as protonation of an internal protonatable group at the catalytic site. Proton uptake from the bulk solution is observed (using pH-sensitive dyes) with the same time constant as that of the $\mathbf{P_R} \rightarrow \mathbf{F}$ transition at the catalytic site (for a summary of the reaction of the *R. sphaeroides* C*c*O with O_2, see Ref. [40]). The proton-transfer reaction has been shown to take place in two distinct steps; the proton is first donated by Glu(I-286) within the D-proton pathway with a time constant of ~ 100 μs, followed by reprotonation of the Glu with a time constant <100 μs at pH 7 [41–43].

A proton-uptake time constant of <100 μs at pH 7 corresponds to a second-order rate constant of $>1 \times 10^{11}$ M^{-1} s^{-1}, i.e., exceeding that of a diffusion-controlled proton transfer to a single protonatable group. A larger than expected proton-uptake rate was also observed at high pH [43], as described briefly below. The apparent pK_A of Glu(I-286) (determined from the pH dependence of the formation rate of state **F**) was found to be 9.4 [43]. Thus, above pH 9.4 a major fraction of Glu(I-286) is unprotonated and the proton is transferred directly from the bulk solution to the proton acceptor at the catalytic site ($\mathbf{P_R} \rightarrow \mathbf{F}$ transition). The protonation of the proton acceptor at the catalytic site and the proton uptake from the bulk solution were investigated independently by following absorbance changes specific to the $\mathbf{P_R} \rightarrow \mathbf{F}$ transition and absorbance changes of a pH-indicator dye in solution, respectively. At pH 9.8, a proton uptake rate constant of ~ 3×10^3 s^{-1} was observed [43], which corresponds to a second-order rate constant of ~ 2×10^{13} M^{-1} s^{-1}. The possibility that direct proton donation from the dye (see below) in solution was rate-limiting was excluded since the extent and rate of formed **F** intermediate were the same in a buffer-free solution as with 40 μM dye or 50 mM buffer.

A theoretical analysis [44] of proton-uptake reactions in C*c*O, coupled to electron transfer between haems *a* and a_3 in the absence of O_2 [15], also revealed an apparent second-order rate constant, 5×10^{11} M^{-1} s^{-1}, exceeding that of a diffusion-controlled proton transfer.

2.2. Bacterial photosynthetic RCs

In bacterial RCs, the first electron transfer from Q_A^- to Q_B, $k_{AB}^{(1)}$, can be measured as a shift in the optical spectrum of the bacteriopheophytin [45] in response to a laser flash. The rate constant $k_{AB}^{(1)}$ is ~ 5×10^3 s^{-1} (to ~ 10^4 s^{-1}, depending on experimental conditions, see, e.g. Refs. [46,47]) at pH 8, and decreases with increasing pH with a p$K_A \cong 8.5$ (or slightly higher, see, e.g. Ref. [47]), due to titration of Glu(L-212) [23]. Proton uptake occurs simultaneously with the electron transfer, as measured using pH-sensitive dyes in the bulk solution (see, e.g. Refs. [24,48]). The $k_{AB}^{(1)}$ reaction in native RCs has been modelled [35] in terms of a rapid proton equilibration between the bulk solution and Glu(L-212), followed by electron transfer that is rate-limited by a conformational change (conformationally gated electron transfer) [49]. Thus, it should be noted that in native RCs, the observed rate constants of proton uptake due to formation of Q_B^-, corresponding to apparent bimolecular rate constants of 5×10^{11}–8×10^{12} M^{-1} s^{-1}, are still not limited by the proton-transfer reaction.

Similar rate constants for proton uptake are observed if the Q_B site is occupied by an inhibitor so that the proton uptake occurs as a response to formation of Q_A^-, which interacts electrostatically with the same protonatable residues as Q_B^- [50], mainly Glu(L-212) at pH>8 [22,24,51,52]. A detailed study of this proton uptake reaction [53] showed that at a specific pH, the observed rate constants were the same with different indicator dyes having different pK_As and hence not dependent on the concentration of the protonated form of the dye, which indicates that direct proton donation from the dye is not rate-limiting.

2.3. Surface modifications affecting proton-transfer reactions

The rapid proton-uptake reactions described above in C*c*O and RCs have been shown to be affected by modifications of the protein surface, indicating a role for surface residues in rapid proton conduction. These surface modifications are discussed in detail below.

2.4. The effect of divalent metal binding to protein surfaces—a tool to investigate proton transfer

Zinc ions (and in some cases also other divalent metal ions) have been shown to inhibit proton-transfer reactions in several membrane-bound enzymes such as the mitochondrial bc_1 complex [54], voltage-gated proton channels [55], photosynthetic RCs [28,29] and on both the proton input and output sides of respiratory oxidases [56–61].

A determination of the X-ray crystal structure of the RCs with bound zinc ions [28] showed that Zn^{2+} was coordinated by His(H-126), His(H-128) and Asp(H-124) (see Fig. 2B). These residues are located at the surface of the RC on the H subunit, at the entry point of one of the previously proposed pathways for proton transfer from the N-side solution into the Q_B-site. This arrangement of His residues and carboxylates is also often found around the input sites of other proton pathways (c.f. detailed discussion below). The results with the RCs indicated that with a metal bound to these residues, proton transfer into the RC was slowed by at least an order of magnitude and was now rate-limiting for both electron transfer reactions ($k_{AB}^{(1)}$ and $k_{AB}^{(2)}$) [29,35]. These results defined the entry point for protons into the RC (Fig. 2B).

With C*c*O from *R. sphaeroides* one Zn^{2+}-binding site was reported to be located near the entry point of the D-pathway, where a cluster of His and Asp residues is found (Fig. 1C). In the presence of Zn^{2+} the proton uptake from bulk solution during the $\mathbf{P_R} \rightarrow \mathbf{F}$ transition, with an intrinsic time constant of <100 μs (see above), was slowed to ~ 2 ms, i.e., by a factor of >20 [60,61].

2.5. Site-specific mutagenesis and other modifications of surface residues

The inhibitory effect by metal ion binding to His(H-126), His(H-128) and Asp(H-124) on proton transfer to the Q_B site in RCs was proposed to be due to the loss of the imidazole groups of the His as initial proton donors in the proton-transfer pathway [29,35]. This proposal was supported by studies on RCs where the two surface His residues were exchanged for alanines using site-directed mutagenesis, showing that in the double His mutant RC, both electron transfer reactions to Q_B were slowed because they were, in contrast to the situation in native RCs, limited by proton uptake from solution [63]. In addition, it was shown that rapid proton uptake rates could be restored ("rescued") by the addition of exogenous proton donors such as imidazole to the bulk solution [63,64]. In contrast to native RCs, in the double His mutant RC the background proton uptake rate in the absence of exogenous donors was close to that corresponding to a direct transfer of H_3O^+ from solution to a specific site at the entrance of the pathway (the apparent bimolecular rate constant was 1.6×10^{11} M^{-1} s^{-1}). These results indicate an important role for the surface histidines, either as proton donors to the pathway or as connectors between the beginning of the pathway and the cluster of other protonatable residues on the surface, as discussed below.

In C*c*O several of the His residues around the entry point of the D-pathway are found at subunit III of the *R. sphaeroides* C*c*O. This subunit does not contain any redox-active cofactors and can be removed without disturbing the structure of the remaining subunits. The removal of SU III resulted in a slowed proton uptake during the $\mathbf{P_R} \rightarrow \mathbf{F}$ transition from <100 μs to ~ 1 ms [65], i.e. by about the same factor as upon Zn^{2+} binding, which also indicates that the protein surface around the entry point of the D-pathway participates in extending the effective radius of the "proton-collecting" domain.

3. Mechanisms of protonation of surface-bound protonatable groups

Protons may be transferred to the entry point of a proton pathway, e.g. a protonatable group, by way of different mechanisms (see Fig. 3):

(i) protons may diffuse to the surface group
(ii) protons may be donated by neighbouring surface groups

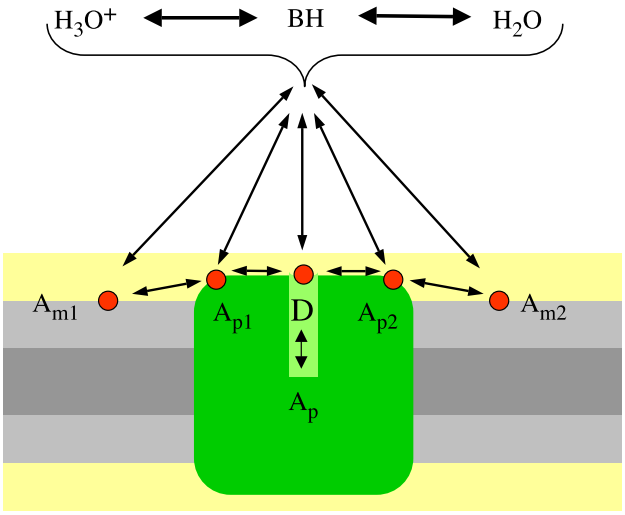

Fig. 3. A summary of the various mechanisms by which protons can be donated to a protonatable group (D) at the orifice of a proton pathway leading to an acceptor within the protein (A_p). Protons from solution may be donated to D, or to proton acceptors at the membrane (A_m) or the protein surface (A_p) by diffusion of hydronium ions (H_3O^+), buffer/pH dye (BH) or water. The surface-bound proton acceptors, A_x, are in rapid equilibrium with D.

(iii) a buffer or dye may donate protons to the surface group
(iv) a water molecule may act as the initial proton donor to the surface group.

The actual mechanism in a specific case may depend on factors such as, e.g. the concentration, charge, pK_A and size of the buffer/dye, the pH, the pK_As and distribution of the proton-accepting groups, the ionic strength (c.f. screening of charges), the geometry of the surface and the local electrostatic field. Below, we discuss each of the mechanisms (i–iv) in detail.

3.1. Proton diffusion to the protein or membrane surface

The process of protonation of a neutral surface group by a proton is described by:

$$k_H = \frac{4\pi N_A R_0 (D_H + D_B)}{1000} \quad (3)$$

in which (units in parentheses) N_A is Avogadro's number $\{mol^{-1}\}$, R_0 is the distance between the proton and the base at which a bond is formed (collision distance, may also be viewed as the effective radius of the base) {cm} and, D_H and D_B are the diffusion coefficients of the proton and the base, respectively $\{cm^2\ s^{-1}\}$. Since in the case of a protein surface-bound base, $D_H \gg D_B$, the rate of encounter of the proton with the base is determined by the diffusion constant of the proton ($D_H = 9.3 \times 10^{-5}$ cm^2 s^{-1} in pure water). The collision distance, R_0, is typically ~ 6 Å. Thus, using these numbers, a value for the second-order rate constant, k_H, of $\sim 4 \times 10^{10}$ M^{-1} s^{-1} is obtained.

In the case of a negatively charged surface-bound group, the process of protonation of the group can be visualised in terms of the group providing an electrostatic field that attracts the proton. The interaction distance of a fixed protein-bound group with the proton is defined as the distance at which the electrostatic Coulomb interaction energy equals the thermal energy (k_BT), defining a so-called "Coulomb cage" around the surface-bound ion. The time required for the proton to find the proton-accepting group is longer than the penetration of the Coulomb cage and bond formation, where the second-order protonation rate, k_H, is described by the Debye–Smoluchowski equation [4,5]:

$$k_H = \frac{4\pi N_A R_0 (D_H + D_B)}{1000} \times \frac{\delta}{e^{\delta} - 1} \times \exp\left(\delta \frac{\kappa R_0}{1 + \kappa R_0}\right) \quad (4)$$

where the first factor is the same as in Eq. (3), and the second and third factors take into account the electrostatic interactions between the base and the proton, where the second factor is the contribution from the electrostatic potential at zero ionic strength and the third factor accounts for the ionic screening. Here δ is the ratio of the Coulomb cage (see definition above), R_C, and the collision distance, R_0,

$$\delta = \frac{Z_H Z_B}{|Z_H Z_B|} R_C / R_0, \quad (5)$$

where,

$$R_C = \frac{|Z_H Z_B| e_0^2}{4\pi\varepsilon_r \varepsilon_0 k_B T} \text{ for } \kappa^{-1} > R_C \ (\kappa \text{ is defined below}) \quad (6)$$

in which Z_HZ_B is the product of the proton and base charges, ε_0 and ε_r are the permittivity in vacuum and the dielectric constant of the medium, respectively, k_B is the Boltzmann constant, e_0 is the elementary charge and T is the temperature. The sign of δ ($Z_HZ_B/|Z_HZ_B|$) is negative or positive for an attractive or repulsive potential, respectively. Using $\varepsilon_r = 78$ (pure H_2O) the value of R_C is ~ 7 Å, which means that for a negatively charged group with $Z_B = -1$ interacting with a proton ($Z_H = +1$), $\delta \cong -1$ (since $R_0 \cong 6$ Å). The absolute value of δ increases with decreasing dielectric constant, i.e., $\delta < -1$, which may be relevant near a protein surface. For an attractive potential, for values of $\delta < -2$, the value of the denominator in $\delta/(e^{\delta} - 1)$ is ~ -1 and thus the factor increases approximately linearly with $|\delta|$. A maximum realistic value for this factor is ~ 10, but normally smaller values are expected [66].

The last factor in Eq. (4) accounts for the effect of ionic screening, where κ^{-1} is the Debye length, i.e. the effective radius of the charge atmosphere surrounding the ion:

$$\kappa^{-1} = \sqrt{\frac{\varepsilon_r \varepsilon_0 k_B T}{2 e_0^2 N_A I}} \quad (7)$$

where I is the ionic strength. If $\kappa^{-1} < R_C$ then R_C should be replaced by the Debye length. The limiting value at which $\kappa^{-1} = R_C$ (7 Å) is obtained is ~ 200 mM monovalent salt solution. For a decreasing κ^{-1} (i.e. increasing ionic strength) the product of the last two factors in Eq. (4) approaches a value of 1, i.e. k_H approaches a value of $\sim 4 \times 10^{10}\ M^{-1}\ s^{-1}$ (i.e. the effect of the attractive electrostatic field vanishes).

The discussion above refers to the protonation rate of a single site. If several surface-bound, rapidly exchanging, negatively charged groups are located near each other at the protein surface, the collective properties of the surface may act to increase the protonation rate of a specific group (e.g. at the entry point of a proton-transfer pathway of a membrane-bound protein). This phenomenon has been termed "the antenna effect", and may give rise to apparent protonation rates of a single site exceeding that of proton diffusion (see below).

3.2. The proton-collecting antenna and proton diffusion along the surface

As discussed above, the proton-collecting antenna is assumed to be composed of nearby negatively charged residues, with overlapping Coulomb cages. In addition to extending the capture radius for protons in solution, the design also facilitates rapid proton exchange between the groups, which results in accelerated protonation rates for each of the components of the antenna [5,7,66,67]. In the case of overlapping Coulomb cages at zero ionic strength, the probability of proton transfer between two negatively charged surface-bound groups rather than proton release to the bulk solution has been estimated to be ~ 1 if the groups are located at a distance of < 12 Å [7,66]. Peitzsch et al. [68] calculated the electrostatic potential around a number of charges localised at membrane surfaces in a solution containing 100 mM of a monovalent salt. They found that when the charges are spaced at a distance of ~ 25 Å there is no overlap of the Coulomb cages (kT equipotential surface, $T = 25$ °C) and around each charge the Coulomb cage has the shape of an ellipsoid extending ~ 5 Å into solution and a radius of ~ 7 Å along the membrane/protein–water interface. An increase in the charge density to an average distance of ~ 16 Å between the charges results in merging of the Coulomb cages forming an approximately equipotential surface extending ~ 7 Å into solution. To move the equipotential surface 12 Å into the solution requires a decrease of the distance between the charges to ~ 8 Å.

The collective negative charge of the surface may increase the apparent protonation rate of a specific surface group beyond the rate corresponding to the diffusion-controlled limit. For example, if a proton is transferred to a specific surface-bound site through a number of other protonatable groups, where these groups can "funnel" protons to the site with (first order) rates exceeding those of protonation of each of the groups through diffusion, then the apparent second-order rate constant for protonation of the site is (at a

maximum) a sum of the diffusion-controlled second-order rate constants for protonation of each of the groups. Therefore, the *apparent* second-order rate constant for protonation of the site may exceed that of proton diffusion, i.e. it can be larger than 4×10^{10} M^{-1} s^{-1} [7,69,70].

The discussion above shows that the effect of the antenna is to accelerate the protonation rate of a specific group and to retain the protons on the surface for times that extend the time constant for deprotonation of a single group. The effect of retaining protons on the surface can be further amplified by the presence of surface-bound protonatable groups displaying higher pK_As, e.g. His residues [7]. For example, the time constant for spontaneous deprotonation to water of a *single* carboxylate having a pK_A of 4.5 is $\sim$ 1 μs while that of a histidine having a pK_A of 6.5 is $\sim$ 100 μs. Note, however, that the proton exchange rate between neighbouring surface-bound groups may be faster and depends on the difference in their pK_As. The discussion above indicates that a protein surface at which His residues are surrounded by carboxylates spaced at distances of <10 Å can efficiently collect protons from solution and retain them for extended times to allow proton uptake through a proton-conducting pathway to, e.g. the catalytic site of an enzyme (Fig. 3).

In a recent theoretical paper Georgievskii et al. [71] modelled the proton-transfer kinetics to the surface of a protein. According to the model, the factor by which a protein surface may enhance the protonation rate of a surface-bound group depends on the ratio of the proton diffusion rate constants in the bulk and on the surface, and the pK_A values and concentration of the surface protonatable groups. Using reasonable values, according to the model, if the surface around the proton pathway entrance is defined by a finite area (with a radius L_{max}) composed of a cluster of protonatable residues, the factor by which the rate is enhanced is determined by the ratio L_{max}/r_0, where r_0 is the radius of the entrance of the proton-transfer pathway. Thus, for a detergent-solubilized protein in solution, even if we assume a connection through protonatable sites of the entire water-exposed surface on the cytoplasmic sides of C*c*O or the RC ($L_{max} \cong 30$ Å, see Fig. 4), and assuming $r_0 = 2-3$ Å, the enhancement factor is a maximum of $\sim$ 15, which may (at the very maximum) bring the apparent diffusion controlled protonation rate to $\sim 10^{12}$ M^{-1} s^{-1}, which is smaller than the observed values of $\sim 10^{13}$ M^{-1} s^{-1} with C*c*O and RCs (see above). However, as suggested to occur in bacteriorhodopsin [72], it is possible that for a multimeric enzyme, the proton-collecting antenna of each molecule might act together to give a larger effective area. To achieve even larger rate constants the protein must be located in a lipid membrane and the radius of this membrane must be included in L_{max}.

Fig. 4 shows the surfaces of the RC and C*c*O around the entry points to the functional proton-transfer pathways. As seen in the figure, there are large numbers of carboxylates and His residues, located within distances of $\sim$ 10 Å from each other, which may act as proton-collecting antennae and extend the proton collecting surface to almost the entire surface area of the protein. In this context, it is possible that the two surface histidines, His(H-126) and His(H-128), shown to be important for proton uptake by the bacterial RCs (see above), are needed to preserve the connectivity of a larger "antenna" around the proton pathway entrance. This scenario could be tested experimentally by mutating protonatable surface residues beyond the two histidines.

3.3. Buffer or pH indicator dye as the proton donor

A proton needed at the catalytic site of a protein might initially be transferred internally from a surface group

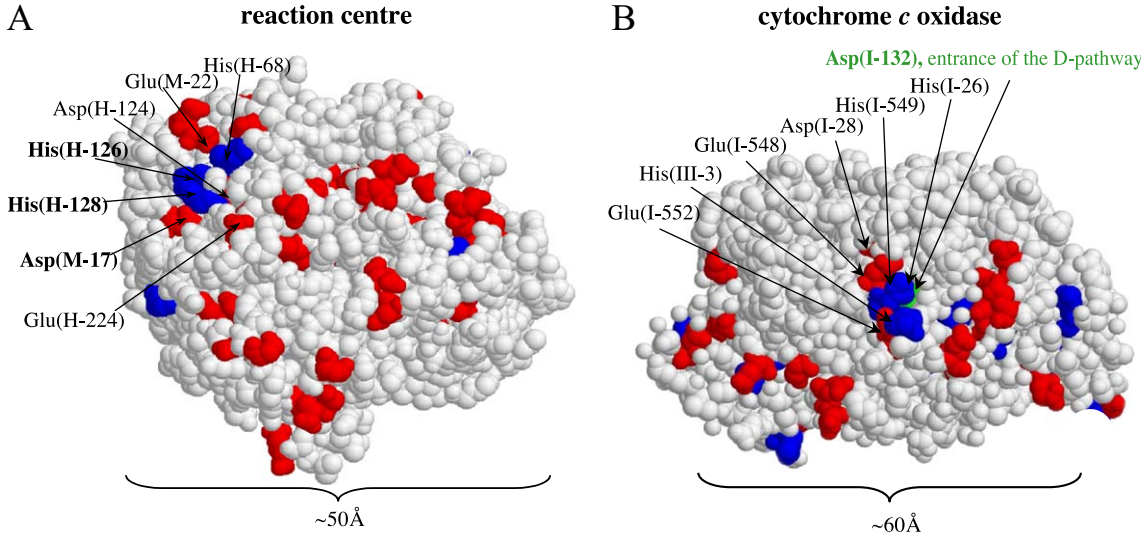

Fig. 4. The surfaces of the RC (A) and C*c*O (B). Acidic and His residues are shown in red and blue, respectively. For the RC, His(H-126) and His(H-128) (in bold) constitute the entry-point for protons. For the C*c*O, the entry-point is Asp(1–132) (in green). Both views are from the cytoplasm.

creating a 'proton hole', i.e. a base (B) at the surface. This base would then be reprotonated from a buffer or dye (D) molecule in solution, in a reaction that according to the Brönsted relation [73] depends on the difference in pK_As of the base and the dye, $\Delta pK_A = pK_A(B) - pK_A(D)$, such that in the range $\Delta pK_A < 0$, the rate increases by a factor of 10 per ΔpK_A unit, and at $pK_A(B) \cong pK_A(D)$, the rate saturates at a constant diffusion-limited value that for a small buffer or dye molecule is $\leq 10^9\ M^{-1}\ s^{-1}$ (for a review see Ref. [1]).

The actual protonation rate of a surface group may also depend on factors such as the geometry of the surface, the structure, charge and pK_A of the dye/buffer as well as the pK_A of the proton acceptor (see above). Therefore, even at high driving force ($\Delta pK_A > 0$, see above) the rate may saturate at a fixed, dye/buffer-concentration independent rate that is smaller than that corresponding to $10^9\ M^{-1}\ s^{-1}$. For example, in the mutant RCs discussed above in which the two surface-bound His residues were removed, proton donation from the bulk solution was rate-limiting for the proton-coupled electron transfer ($k_{AB}^{(1)}$) reaction [63]. In this case, addition of 40 μM of a dye with a $pK_A \cong pH \cong 9$ (so that about 20 μM of the dye was protonated) did not increase the proton donation rate to the pathway entrance (where the immediate proton acceptor was modelled to have a $pK_A \cong 3-5$ [64]) above the background of $\sim 200\ s^{-1}$, which in this specific situation puts an upper limit on the apparent second-order rate constant of $\sim 10^7\ M^{-1}\ s^{-1}$.

The concept of a proton-collecting antenna can also be applied when a buffer or a pH-indicator dye is the donor. If a proton is delivered to a surface group that is in rapid equilibrium with the surrounding groups, and proton diffusion along the surface is rapid compared to the escape rate of the proton to the bulk solution, a specific surface group may be protonated with an apparent rate exceeding the diffusion-controlled limit.

At pH 7 the concentration of free protons in water is only 0.1 μM, which corresponds to a protonation rate of a surface base of $\sim 4 \times 10^3\ s^{-1}$ (using a second-order rate constant of $4 \times 10^{10}\ M^{-1}\ s^{-1}$). Thus, even though the diffusion coefficient of the dye/buffer molecules is much smaller than that of protons, if dye/buffer is present, at optimal conditions (i.e. the second-order rate constant is $10^9\ M^{-1}\ s^{-1}$; see above) it may already at a concentration of 1 μM act as a proton donor to the surface groups with the same rate as that of direct protonation of the group. In principle, if the dye is the proton donor, the proton-uptake rate should depend on the dye concentration. However, it may be difficult to experimentally determine whether or not protons are delivered to the surface through exchange with the dye by varying the dye concentration. To illustrate this problem we consider a reaction within an enzyme that displays a rate constant of $10^4\ s^{-1}$, which is associated with proton uptake from the bulk solution. If the dye acts as the proton donor, the observed rate would be independent of the dye concentration at concentrations of >10 μM dye (for a diffusion-controlled second-order rate constant of $10^9\ M^{-1}\ s^{-1}$) and decrease at lower concentrations because the overall reaction is rate-limited by the chemical reaction with a rate of $10^4\ s^{-1}$ within the enzyme. However, for the pH indicator dyes often used, typically dye concentrations of 10–100 μM must be used to obtain an adequate signal-to-noise ratio. Thus, in the dye concentration range in which the rate decreases with decreasing dye concentration, the signal-to-noise ratio may be too low to enable measurements of the kinetics of proton uptake.

Another problem that may be encountered when comparing proton-uptake rates in single-turnover experiments with overall turnover rates is illustrated in the following example. As discussed above, the results from (single turnover) studies of native RCs and C*c*Os showed that the observed proton-uptake rates were independent of the dye/buffer concentration and that the rates of the proton-coupled electron-transfer reactions did not change in the absence of a dye. These results may be explained to indicate that both in the presence and absence of a dye/buffer, the rates of electron and proton transfer are the same. However, an alternative scenario is that the electron-transfer reaction occurs upon proton transfer from a surface group (which in the case of RCs would be the surface His discussed above) to an internal group through a proton-transfer pathway. In the absence of a dye or buffer, the reprotonation of the base that is formed at the surface as a result of the proton transfer is slower than the internal proton transfer. When a dye is added to *study proton uptake from solution* (typically at concentrations of 10–100 μM, as indicated above), it is present at high enough concentrations to reprotonate the "hole" more rapidly than the hole is formed. This example shows that in some cases it may be difficult to access the true rate of direct proton transfer from the bulk solution to the protein surface in the absence of a dye or buffer. However, if the ultimate proton donation from the bulk solution to reprotonate the hole is rate-limiting for the overall catalytic reaction, under steady-state conditions, the local, surface-bound proton buffer will be depleted of protons and the overall rate is expected to be slower without than with a buffer or dye, which makes it possible to access the mechanism experimentally.

3.4. Water as a proton donor

In a number of studies, water has been considered as the primary proton donor to a base at the surface [4,53,74] that is formed upon proton transfer to an intraprotein proton acceptor. For example, in a recent study Gopta et al. [74] studied proton transfer upon reduction of the Q_B site in chromatophores containing photosynthetic RCs. They were able to independently measure the rates of three different events: (1) the electron transfer to Q_B, (2) the proton-transfer to residues around the Q_B site, triggered by the formation of Q_B^- and (3) the proton uptake from the bulk solution. The results showed that formation of Q_B^- with a time constant of ~ 100 μs was associated with proton transfer from surface

groups to the Q_B site with the same time constant, i.e. without any measurable delay. However, the reprotonation of the surface groups from the bulk solution was delayed and displayed a time constant of ~400 μs. It might be worth noting that this delay is not observed in isolated RCs, where proton uptake from bulk solution is concomitant with Q_B^- formation (described in the RC section above), which might relate to the accessibility of the dye to the surface, as discussed above. Gopta et al. [74] found that the rate of proton donation was independent of the pH indicator dye concentration (at <500 μM dye) and that it was not accelerated by the addition of buffer (at concentrations in the range 10–60 μM), which excludes the possibility of proton donation by the dye or buffer. The rate of proton donation by water, $3 \times 10^{10 + pK_A(B) - 14}$ s^{-1}, is within a factor of 10 the same as that of proton diffusion at pH 6.5. To distinguish between the two mechanisms, Gopta et al. [74] compared the Arrhenius activation energies for the two processes and concluded that in the experimental system that they investigated water was the immediate proton donor to the protein surface groups.

According to the above described scenario, proton transfer from water to a base (B^-) at the surface, formed upon proton transfer to an intraprotein acceptor (A_p^-), is followed by reprotonation of the hydroxide from the bulk solution, e.g. by a buffer or dye (D):

$$A_p^- + BH \underset{k_{-1}}{\overset{k_1}{\rightleftarrows}} A_pH + B^- \quad (8a)$$

$$H_2O + B^- \underset{k_{OH}}{\overset{k_B}{\rightleftarrows}} OH^- + BH \quad (8b)$$

$$OH^- + DH \underset{k_D}{\overset{k_{OH}}{\rightleftarrows}} H_2O + D^- \quad (8c)$$

The second-order rate constant for protonation of B^- is given by:

$$k_B = k_{OH} \times 10^{pK_A(B) - pK_A(H_2O)} \ \{M^{-1}s^{-1}\} \quad (9)$$

where $pK_A(H_2O) \cong 15.7$ and k_{OH} is 3×10^{10} M^{-1} s^{-1} [75]. Taking into account the concentration of water (i.e. multiplying k_B in Eq. (9) by 55.5 M), the first-order rate constant, k_B' is:

$$k_B' = k_{OH} \times 10^{pK_A(B) - 14} = 3 \times 10^{10 + pK_A(B) - 14} \ \{s^{-1}\} \quad (10)$$

According to Eq. (10), the rate is determined by the pK_A of the acceptor base. Thus, in the case of a single group, at pH values below the pK_A of the base (i.e. the base is protonated before it transfers its proton to A_p^-), the proton-uptake rate is expected to be pH-independent. If, on the other hand, we assume that a protein surface is composed of a large number of rapidly (i.e. the equilibration among the groups is faster than their protonation from the bulk solution) exchanging protonatable groups with different pK_As displaying a continuous spectrum of pK_As, then all groups having a pK_A>pH are protonated before the proton transfer from BH to A_p^- (Eq. (8a)). Thus, the formed base B^- will be the one having the lowest pK_A of those that were protonated, i.e., the group has a pK_A=pH. Thus, at any given pH, the proton-uptake rate k_B' is:

$$k_B' = 3 \times 10^{10 + pH - 14} \ s^{-1} \quad (11)$$

Under the assumptions above, according to Eq. (11) the rate of proton transfer from water to the base would increase with increasing pH because the driving force for proton transfer increases with increasing pK_A of the surface acceptor base. Even though this pH dependence may be weaker than that obtained from Eq. (11) (if there is a small number of surface groups), often the observed rates of proton transfer (e.g. of the reactions in RCs and C*c*Os discussed above) do not increase, but rather decrease with increasing pH. Thus, these reactions cannot be rate-limited by deprotonation of water. However, since the rate of proton transfer from H_2O to a base is relatively high above pH 7 (>3×10^3 s^{-1}), the proton-transfer reactions can still take place through transient proton donation by H_2O, but be rate-limited by other events.

4. The role of the protein surface in proton release

An issue directly related to proton uptake by a membrane-bound protein is that of the kinetics of proton release from a proton pump to solution. For a single group, the rate constant (k_{off}) for spontaneous proton release to bulk H_2O depends on the pK_A of the group. Assuming a k_{on} of 4×10^{10} M^{-1} s^{-1}, k_{off} is $4 \times 10^{(10 - pK_A)}$ s^{-1}, which means that a group having a pK_A of 7.5 would release its proton with a time constant of ~1 ms while a group with a pK_A of 4.5 would release the proton with a time constant of ~1 μs. The issue of a delayed proton release is related to that of a proton-collecting antenna discussed above in connection with proton uptake. A delayed proton release is expected in cases when an array of amino acid residues, i.e. a local, fixed buffer, is present at the exit point of a proton-transfer pathway [76]. A proton that is released into the matrix of fixed buffer groups at the protein surface may either be transferred to a neighbouring group or to the bulk solution. The probability for the proton of being released to the bulk solution depends on the relative rates of the two processes. If the proton-transfer rate between the surface groups is rapid compared to the release rate, the proton is likely to be transferred among the surface protonatable groups before it is released to the bulk solution, which results in a delayed proton release. As discussed in the previous section, if the surface is composed of a large number of protonatable groups with a distribution of pK_As, the proton is expected to end up at a group having the highest pK_A of those that are

not protonated at the given pH, i.e., $pK_A = pH$. Thus, at pH 7.5 the proton release time constant would be ~ 1 ms.

Several research groups have reported results from studies of proton-transfer kinetics along membrane fragments containing membrane-bound proteins. For example, the results from the studies of bacteriorhodopsin [77–80] showed that a pH indicator that was attached to the protein surface on the same side of the membrane where the proton is released became protonated with a time constant of ~ 100 μs. The same time constant was observed when the pH indicator was moved to the opposite side of the membrane. However, a pH indicator dye present in the bulk solution responded on a much slower time scale displaying a time constant of ~ 1 ms. It was concluded that proton conduction in the interface between the protein surface and the bulk solution is faster than the equilibration with the bulk solution [77]. As an alternative, it was also suggested that the delayed proton release may be a consequence of rapid proton equilibration among the surface groups ([81], but see Ref. [74]) or through water being the immediate acceptor, where the formed H_3O^+ then slowly protonates the pH dye in the bulk solution ([74], see also Ref. [82]).

In analogy with the discussion above, a pH-dye or buffer in solution may also act to accelerate proton release from the matrix of surface-bound protonatable groups to the bulk solution. As discussed above, the rate of proton exchange is determined by the properties of the dye/buffer and the difference in the pK_As of the proton donor and acceptor. Also in this case the presence of surface-bound protonatable groups may either delay (if the probability is larger to transfer the proton along the surface than to the buffer and/or the group to which the proton is transferred has a high pK_A) or accelerate (if the proton is released to a low-pK_A group) proton release to the bulk solution.

In C*c*O, proton release to the bulk solution on the P-side, measured time-resolved using pH dyes, was observed on the time scale of the $\mathbf{F} \rightarrow \mathbf{O}$ ($\tau \cong 1$ ms at pH 7), but not during the $\mathbf{P_R} \rightarrow \mathbf{F}$ ($\tau \cong 100$ μs at pH 7) transition [83]. Yet, electrogenic events attributed to the transmembrane translocation of protons were observed for both transitions. Thus, also in this system a delay of proton release is possible, although it cannot be excluded that there may be alternative explanations of the experimental results (Gilderson et al., manuscript in preparation).

5. Summary

As evident from this summary, the interface between a membrane protein and the bulk water solution plays an important role in the dynamics of proton uptake and release thereby controlling the reactions catalysed by (within) membrane-bound enzymes. The experimental and theoretical studies of these processes have greatly benefited from the recent advancements in determination of high-resolution X-ray structures of a number of membrane proteins. However, to understand the basic mechanisms of proton transfer between the bulk water solution and the interior of a membrane-bound protein, the structural information must be combined with a detailed mechanistic understanding of proton transport at and through the interface, i.e., the confined space between the surface and the bulk solution, and the bulk solution itself. These aspects have been considered and investigated by combining the structural information with the use of site-specific mutagenesis, rapid time-resolved spectroscopic techniques and theory. In this review we have summarised a number of possible mechanisms by which protons are transferred from water solution to the mouth of proton-transfer pathways, exemplified by results from studies of C*c*Os and photosynthetic RCs. Each of these mechanisms depends on the presence of specific surface groups that accept/abstract protons from water, buffer molecules (pH dyes) or hydronium ions, where the collective properties of the protein–membrane surface may act to increase the proton-collecting surface area and to provide a wide range of rapidly exchanging groups, each optimised to become protonated at specific conditions. Although we still need a unified view on the molecular events associated with rapid proton transfer from the bulk solution to the interior of membrane proteins, there has been great progress in the understanding of proton-transfer reactions at the membrane–protein-solution interface at the molecular level.

Acknowledgements

We are indebted to Menachem Gutman, Armen Mulkidjanian, Esther Nachliel, Mark Paddock, Alexei Stuchebrukhov and Colin Wraight for discussions, and for giving valuable comments on this manuscript.

References

[1] T.E. Decoursey, Voltage-gated proton channels and other proton transfer pathways, Physiol. Rev. 83 (2003) 475–579.
[2] M. Eigen, Proton transfer, acid–base catalysis, and enzymic hydrolysis: I. Elementary processes, Angew. Chem. 75 (1963) 489–508.
[3] R.P. Bell, The Proton in Chemistry, 2nd ed., Chapman and Hall, London, 1973.
[4] M. Gutman, E. Nachliel, The dynamic aspects of proton-transfer processes, Biochim. Biophys. Acta 1015 (1990) 391–414.
[5] M. Gutman, E. Nachliel, Time-resolved dynamics of proton transfer in proteinous systems, Annu. Rev. Phys. Chem. 48 (1997) 329–356.
[6] Y. Marantz, E. Nachliel, A. Aagaard, P. Brzezinski, M. Gutman, The proton collecting function of the inner surface of cytochrome *c* oxidase from *Rhodobacter sphaeroides*, Proc. Natl. Acad. Sci. U. S. A. 95 (1998) 8590–8595.
[7] V. Sacks, Y. Marantz, A. Aagaard, S. Checover, E. Nachliel, M. Gutman, The dynamic feature of the proton collecting antenna of a protein surface, Biochim. Biophys. Acta 1365 (1998) 232–240.
[8] S. Iwata, C. Ostermeier, B. Ludwig, H. Michel, Structure at 2.8 Å resolution of cytochrome *c* oxidase from *Paracoccus denitrificans*, Nature 376 (1995) 660–669.

[9] C. Ostermeier, A. Harrenga, U. Ermler, H. Michel, Structure at 2.7 Å resolution of the *Paracoccus denitrificans* two-subunit cytochrome *c* oxidase complexed with an antibody FV fragment, Proc. Natl. Acad. Sci. U. S. A. 94 (1997) 10547–10553.
[10] T. Tsukihara, H. Aoyama, E. Yamashita, T. Tomizaki, H. Yamaguchi, K. Shinzawa-Itoh, R. Nakashima, R. Yaono, S. Yoshikawa, The whole structure of the 13-subunit oxidized cytochrome *c* oxidase at 2.8 Å [see comments], Science 272 (1996) 1136–1144.
[11] S. Yoshikawa, K. Shinzawa-Itoh, R. Nakashima, R. Yaono, E. Yamashita, N. Inoue, M. Yao, M.J. Fei, C.P. Libeu, T. Mizushima, H. Yamaguchi, T. Tomizaki, T. Tsukihara, Redox-coupled crystal structural changes in bovine heart cytochrome *c* oxidase, Science 280 (1998) 1723–1729.
[12] S. Ferguson-Miller, G.T. Babcock, Heme/copper terminal oxidases, Chem. Rev. 96 (1996) 2889–2907.
[13] D. Zaslavsky, R.B. Gennis, Proton pumping by cytochrome *c* oxidase: progress, problems and postulates, Biochim. Biophys. Acta 1458 (2000) 164–179.
[14] A.A. Konstantinov, S. Siletsky, D. Mitchell, A. Kaulen, R.B. Gennis, The roles of the two proton input channels in cytochrome *c* oxidase from *Rhodobacter sphaeroides* probed by the effects of site-directed mutations on time-resolved electrogenic intraprotein proton transfer, Proc. Natl. Acad. Sci. U. S. A. 94 (1997) 9085–9090.
[15] P. Brzezinski, P. Ädelroth, Pathways of proton transfer in cytochrome *c* oxidase, J. Bioenerg. Biomembranes 30 (1998) 99–107.
[16] M. Ruitenberg, A. Kannt, E. Bamberg, B. Ludwig, H. Michel, K. Fendler, Single-electron reduction of the oxidized state is coupled to proton uptake via the K pathway in *Paracoccus denitrificans* cytochrome *c* oxidase, Proc. Natl. Acad. Sci. U. S. A. 97 (2000) 4632–4636.
[17] M. Wikström, A. Jasaitis, C. Backgren, A. Puustinen, M.I. Verkhovsky, The role of the D- and K-pathways of proton transfer in the function of the haem-copper oxidases, Biochim. Biophys. Acta 1459 (2000) 514–520.
[18] M.Y. Okamura, M.L. Paddock, M.S. Graige, G. Feher, Proton and electron transfer in bacterial reaction centers, Biochim. Biophys. Acta 1458 (2000) 148–163.
[19] R.E. Blankenship, M.T. Madigan, C.E. Bauer, Anoxygenic Photosynthetic Bacteria, Kluwer Academic Publishing, Dordrecht, The Netherlands, 1995.
[20] C.A. Wraight, Proton and electron transfer in the acceptor quinone complex of photosynthetic reaction centers from *Rhodobacter sphaeroides*, Front. Biosci. 9 (2004) 309–337.
[21] M.S. Graige, M.L. Paddock, G. Feher, M.Y. Okamura, Observation of the protonated semiquinone intermediate in isolated reaction centers from *Rhodobacter sphaeroides*: implications for the mechanism of electron and proton transfer in proteins, Biochemistry 38 (1999) 11465–11473.
[22] E. Takahashi, C.A. Wraight, Proton and electron transfer in the acceptor quinone complex of *Rhodobacter sphaeroides* reaction centers: characterization of site-directed mutants of the two ionizable residues, GluL212 and AspL213, in the Q_B binding site, Biochemistry 31 (1992) 855–866.
[23] M.L. Paddock, S.H. Rongey, G. Feher, M.Y. Okamura, Pathway of proton transfer in bacterial reaction centers: replacement of glutamic acid 212 in the L subunit by glutamine inhibits quinone (secondary acceptor) turnover, Proc. Natl. Acad. Sci. U. S. A. 86 (1989) 6602–6606.
[24] P.H. McPherson, M. Schönfeld, M.L. Paddock, M.Y. Okamura, G. Feher, Protonation and free energy changes associated with formation of Q_BH_2 in native and Glu-L212 → Gln mutant reaction centers from *Rhodobacter sphaeroides*, Biochemistry 33 (1994) 1181–1193.
[25] G. Fritzsch, L. Kampmann, G. Kapaun, H. Michel, Water clusters in the reaction centre of *Rhodobacter sphaeroides*, Photosynth. Res. 55 (1998) 127–132.
[26] L. Baciou, H. Michel, Interruption of the water chain in the reaction center from *Rhodobacter sphaeroides* reduces the rates of the proton uptake and of the second electron transfer to Q_B, Biochemistry 34 (1995) 7967–7972.
[27] E.C. Abresch, M.L. Paddock, M.H.B. Stowell, T.M. McPhillips, H.L. Axelrod, S.M. Soltis, D.C. Rees, M.Y. Okamura, G. Feher, Identification of proton transfer pathways in the X-ray crystal structure of the bacterial reaction center from *Rhodobacter sphaeroides*, Photosynth. Res. 55 (1998) 119–125.
[28] H.L. Axelrod, E.C. Abresch, M.L. Paddock, M.Y. Okamura, G. Feher, Determination of the binding sites of the proton transfer inhibitors Cd^{2+} and Zn^{2+} in bacterial reaction centers, Proc. Natl. Acad. Sci. U. S. A. 97 (2000) 1542–1547.
[29] M.L. Paddock, M.S. Graige, G. Feher, M.Y. Okamura, Identification of the proton pathway in bacterial reaction centers: inhibition of proton transfer by binding of Zn2+ or Cd2+, Proc. Natl. Acad. Sci. U. S. A. 96 (1999) 6183–6188.
[30] M.L. Paddock, G. Feher, M.Y. Okamura, Identification of the proton pathway in bacterial reaction centers: replacement of Asp-M17 and Asp-L210 with Asn reduces the proton transfer rate in the presence of Cd^{2+}, Proc. Natl. Acad. Sci. U. S. A. 97 (2000) 1548–1553.
[31] M.L. Paddock, P. Ädelroth, C. Chang, E.C. Abresch, G. Feher, M.Y. Okamura, Identification of the proton pathway in bacterial reaction centers: cooperation between Asp-M17 and Asp-L210 facilitates proton transfer to the secondary quinone (Q_B), Biochemistry 40 (2001) 6893–6902.
[32] M.L. Paddock, P.H. McPherson, G. Feher, M.Y. Okamura, Pathway of proton transfer in bacterial reaction centers: replacement of serine-L223 by alanine inhibits electron and proton transfers associated with reduction of quinone to dihydroquinone, Proc. Natl. Acad. Sci. U. S. A. 87 (1990) 6803–6807.
[33] M.L. Paddock, S.H. Rongey, P.H. McPherson, A. Juth, G. Feher, M.Y. Okamura, Pathway of proton transfer in bacterial reaction centers: role of aspartate-L213 in proton transfers associated with reduction of quinone to dihydroquinone, Biochemistry 33 (1994) 734–745.
[34] E. Takahashi, C.A. Wraight, A crucial role for Asp-L213 in the proton transfer pathway to the secondary quinone of reaction centers from *Rhodobacter sphaeroides*, Biochim. Biophys. Acta 1020 (1990) 107–112.
[35] P. Ädelroth, M.L. Paddock, L.B. Sagle, G. Feher, M.Y. Okamura, Identification of the proton pathway in bacterial reaction centers: both protons associated with reduction of Q_B to Q_BH_2 share a common entry point, Proc. Natl. Acad. Sci. U. S. A. 97 (2000) 13086–13091.
[36] L. Gerencsér, G. Laczkó, P. Maróti, Unbinding of oxidized cytochrome *c* from photosynthetic reaction center of *Rhodobacter sphaeroides* is the bottleneck of fast turnover, Biochemistry 38 (1999) 16866–16875.
[37] G.T. Babcock, M. Wikström, Oxygen activation and the conservation of energy in cell respiration, Nature 356 (1992) 301–309.
[38] Ó. Einarsdóttir, Fast reactions of cytochrome-oxidase, Biochim. Biophys. Acta 1229 (1995) 129–147.
[39] P. Brzezinski, G. Larsson, P. Ädelroth, Functional Aspects of Heme-copper Terminal Oxidases, in: D. Zannoni (Ed.), Respiration in Archaea and Bacteria, vol. 1, Kluwer, The Netherlands, 2004 (in press).
[40] P. Ädelroth, M. Ek, P. Brzezinski, Factors determining electron-transfer rates in cytochrome *c* oxidase: investigation of the oxygen reaction in the *R. sphaeroides* and bovine enzymes, Biochim. Biophys. Acta 1367 (1998) 107–117.
[41] I.A. Smirnova, P. Ädelroth, R.B. Gennis, P. Brzezinski, Aspartate-132 in cytochrome *c* oxidase from *Rhodobacter sphaeroides* is involved in a two-step proton transfer during oxo-ferryl formation, Biochemistry 38 (1999) 6826–6833.
[42] P. Ädelroth, M. Karpefors, G. Gilderson, F.L. Tomson, R.B. Gennis, P. Brzezinski, Proton transfer from glutamate 286 determines the transition rates between oxygen intermediates in cytochrome *c* oxidase, Biochim. Biophys. Acta 1459 (2000) 533–539.
[43] A. Namslauer, A. Aagaard, A. Katsonouri, P. Brzezinski, Intramolecular proton-transfer reactions in a membrane-bound proton pump: the

effect of pH on the peroxy to ferryl transition in cytochrome *c* oxidase, Biochemsitry 42 (2003) 1488–1498.
[44] A.I. Kotelnikov, E.S. Medvedev, D.M. Medvedev, A.A. Stuchebrukhov, Kinetic treatment of coupled electron and proton transfer in flash-photolysis experiments on carbon monoxide-inhibited mixed-valence cytochrome *c* oxidase, J. Phys. Chem., B 105 (2001) 5789–5796.
[45] A. Verméglio, R.K. Clayton, Kinetics of electron transfer between the primary and the secondary electron acceptor in reaction centers from *Rhodopseudomonas sphaeroides*, Biochim. Biophys. Acta 461 (1977) 159–165.
[46] L. Gerencsér, P. Maróti, Retardation of proton transfer caused by binding of the transition metal ion to the bacterial reaction center is due to pK(a) shifts of key protonatable residues, Biochemistry 40 (2001) 1850–1860.
[47] J. Miksovska, M. Valerio-Lepiniec, M. Schiffer, D.K. Hanson, P. Sebban, In bacterial reaction centers, a key residue suppresses mutational blockage of two different proton transfer steps, Biochemistry 37 (1998) 2077–2083.
[48] P. Maróti, C.A. Wraight, Flash-induced proton binding by bacterial photosynthetic reaction centers: influence of the redox states of the acceptor quinones and primary donor, Biochim. Biophys. Acta 934 (1988) 329–347.
[49] M.S. Graige, G. Feher, M.Y. Okamura, Conformational gating of the electron transfer reaction $Q_A^- Q_B \rightarrow Q_A Q_B^-$ in bacterial reaction centers of *Rhodobacter sphaeroides* determined by a driving force assay, Proc. Natl. Acad. Sci. U. S. A. 95 (1998) 11679–11684.
[50] J. Miksovska, M. Schiffer, D.K. Hanson, P. Sebban, Proton uptake by bacterial reaction centers: the protein complex responds in a similar manner to the reduction of either quinone acceptor, Proc. Natl. Acad. Sci. U. S. A. 96 (1999) 14348–14353.
[51] E. Nabedryk, J. Breton, R. Hienerwadel, C. Fogel, W. Mäntele, M.L. Okamura, M.Y. Okamura, Fourier transforms infrared difference spectroscopy of secondary quinone acceptor photoreduction in proton transfer mutants of *Rhodobacter sphaeroides*, Biochemistry 34 (1995) 14722–14732.
[52] J. Miksovska, P. Maróti, J. Tandori, M. Schiffer, D.K. Hanson, P. Sebban, Distant electrostatic interactions modulate the free energy level of Q_A^- in the photosynthetic reaction center, Biochemistry 35 (1996) 15411–15417.
[53] P. Maróti, C.A. Wraight, Kinetics of H^+ ion binding by the $P+Q_A^-$ state of bacterial photosynthetic reaction centers: rate limitation within the protein, Biophys. J. 73 (1997) 367–381.
[54] T.A. Link, G. von Jagow, Zinc ions inhibit the Q(P) center of bovine heart mitochondrial bc_1 complex by blocking a protonatable group, J. Biol. Chem. 270 (1995) 25001–25006.
[55] V.V. Cherny, T.E. DeCoursey, pH-dependent inhibition of voltage-gated H^+ currents in rat alveolar epithelial cells by Zn^{2+} and other divalent cations, J. Gen. Physiol. 114 (1999) 819–838.
[56] P. Nicholls, A.P. Singh, Effect of zinc on proteoliposomal cytochrome oxidase, Life Sci. Adv. (Agra, India) 7 (1988) 321–326.
[57] K. Kita, M. Kasahara, Y. Anraku, Formation of a membrane potential by reconstructed liposomes made with cytochrome *b*562-o complex, a terminal oxidase of *Escherichia coli* K12, J. Biol. Chem. 257 (1982) 7933–7935.
[58] A. Kannt, T. Ostermann, H. Muller, M. Ruitenberg, Zn^{2+} binding to the cytoplasmic side of *Paracoccus denitrificans* cytochrome *c* oxidase selectively uncouples electron transfer and proton translocation, FEBS Lett. 503 (2001) 142–146.
[59] D.A. Mills, B. Schmidt, C. Hiser, E. Westley, S. Ferguson-Miller, Membrane potential-controlled inhibition of cytochrome *c* oxidase by zinc, J. Biol. Chem. 277 (2002) 14894–14901.
[60] A. Aagaard, P. Brzezinski, Zinc ions inhibit oxidation of cytochrome *c* oxidase by oxygen, FEBS Lett. 494 (2001) 157–160.
[61] A. Aagaard, A. Namslauer, P. Brzezinski, Inhibition of proton transfer in cytochrome *c* oxidase by zinc ions: delayed proton uptake during oxygen reduction, Biochim. Biophys. Acta 1555 (2002) 133–139.
[63] P. Ädelroth, M.L. Paddock, A. Tehrani, J.T. Beatty, G. Feher, M.Y. Okamura, Identification of the proton pathway in bacterial reaction centers: decrease of proton transfer rate by mutation of surface histidines at H126 and H128 and chemical rescue by imidazole identifies the initial proton donors, Biochemistry 40 (2001) 14538–14546.
[64] M.L. Paddock, P. Ädelroth, G. Feher, M.Y. Okamura, J.T. Beatty, Determination of proton transfer rates by chemical rescue: application to bacterial reaction centers, Biochemistry 41 (2002) 14716–14725.
[65] G. Gilderson, L. Salomonsson, A. Aagaard, J. Gray, P. Brzezinski, J. Hosler, Subunit III of cytochrome *c* oxidase of *Rhodobacter sphaeroides* is required to maintain rapid proton uptake through the D pathway at physiologic pH, Biochemistry 42 (2003) 7400–7409.
[66] M. Gutman, E. Nachliel, The dynamics of proton-exchange between bulk and surface groups, Biochim. Biophys. Acta 1231 (1995) 123–138.
[67] E. Nachliel, S. Yaniv–Checover, M. Gutman, The role of the surface group in funnelling of protons towards the protonic channel of bacteriorhodopsin, Solid State Ionics 97 (1997) 75–82.
[68] R.M. Peitzsch, M. Eisenberg, K.A. Sharp, S. McLaughlin, Calculations of the electrostatic potential adjacent to model phospholipid bilayers, Biophys. J. 68 (1995) 729–738.
[69] M. Gutman, E. Nachliel, A. Mezer, O. Noivirt, Gauging of local micro-environment and protein water interface by time-resolved single-proton transfer reactions, Ann. Eur. Acad. Sci. 1 (2003) 75–107.
[70] B. Schatzler, N.A. Dencher, J. Tittor, D. Oesterhelt, S. Yaniv-Checover, E. Nachliel, M. Gutman, Subsecond proton-hole propagation in bacteriorhodopsin, Biophys. J. 84 (2003) 671–686.
[71] Y. Georgievskii, E.S. Medvedev, A.A. Stuchebrukhov, Proton transport via the membrane surface, Biophys. J. 82 (2002) 2833–2846.
[72] S. Checover, Y. Marantz, E. Nachliel, M. Gutman, M. Pfeiffer, J. Oesterhelt, D. Oesterhelt, N.A. Dencher, Dynamics of the proton transfer reaction on the cytoplasmic surface of bacteriorhodopsin, Biochemistry 40 (2001) 4281–4292.
[73] J.N. Brönsted, K. Pedersen, Z. Phys. Chem. A 108 (1923) 185.
[74] O.A. Gopta, D.A. Cherepanov, W. Junge, A.Y. Mulkidjanian, Proton transfer from the bulk to the bound ubiquinone Q(B) of the reaction center in chromatophores of *Rhodobacter sphaeroides*: retarded conveyance by neutral water, Proc. Natl. Acad. Sci. U. S. A. 96 (1999) 13159–13164.
[75] E. Nachliel, Z. Ophir, M. Gutman, Kinetic-analysis of fast alkalinization transient by photoexcited heterocyclic-compounds: pOH jump, J. Am. Chem. Soc. 109 (1987) 1342–1345.
[76] W. Junge, S. McLaughlin, The role of fixed and mobile buffers in the kinetics of proton movement, Biochim. Biophys. Acta 890 (1987) 1–5.
[77] J. Heberle, J. Riesle, G. Thiedemann, D. Oesterhelt, N.A. Dencher, Proton migration alone the membrane-surface and retarded surface to bulk transfer, Nature 370 (1994) 379–382.
[78] J. Heberle, N.A. Dencher, Surface-bound optical probes monitor proton translocation and surface-potential changes during the bacteriorhodopsin photocycle, Proc. Natl. Acad. Sci. U. S. A. 89 (1992) 5996–6000.
[79] U. Alexiev, R. Mollaaghababa, P. Scherrer, H.G. Khorana, M.P. Heyn, Rapid long-range proton diffusion along the surface of the purple membrane and delayed proton-transfer into the bulk, Proc. Natl. Acad. Sci. U. S. A. 92 (1995) 372–376.
[80] A.K. Dioumaev, H.T. Richter, L.S. Brown, M. Tanio, S. Tuzi, H. Saito, Y. Kimura, R. Needleman, J.K. Lanyi, Existence of a proton transfer chain in bacteriorhodopsin: participation of Glu-194 in the release of protons to the extracellular surface, Biochemistry 37 (1998) 2496–2506.
[81] E. Nachliel, M. Gutman, Quantitative evaluation of the dynamics of proton transfer from photoactivated bacteriorhodopsin to the bulk, FEBS Lett. 393 (1996) 221–225.
[82] D.A. Cherepanov, B.A. Feniouk, W. Junge, A.Y. Mulkidjanian, Low dielectric permittivity of water at the membrane interface: effect on the energy coupling mechanism in biological membranes, Biophys. J. 85 (2003) 1307–1316.

[83] M. Oliveberg, S. Hallén, T. Nilsson, Uptake and release of protons during the reaction between cytochrome *c* oxidase and molecular oxygen: a flow-flash investigation, Biochemistry 30 (1991) 436–440.
[84] M. Svensson-Ek, J. Abramson, G. Larsson, S. Törnroth, P. Brzezinski, S. Iwata, The X-ray crystal structures of wild-type and EQ(I-286) mutant cytochrome *c* oxidases from *Rhodobacter sphaeroides*, J. Mol. Biol. 321 (2002) 329–339.
[85] W. Humphrey, A. Dalke, K. Schulten, VMD: visual molecular dynamics, J. Mol. Graph. 14 (1996) 33.
[86] M.H. Stowell, T.M. McPhillips, D.C. Rees, S.M. Soltis, E. Abresch, G. Feher, Light-induced structural changes in photosynthetic reaction center: implications for mechanism of electron-proton transfer, Science 276 (1997) 812–816.